5.3-GHz MIMO Radio Channel Sounder

Veli-Matti Kolmonen, Jarmo Kivinen, Lasse Vuokko, and Pertti Vainikainen, *Member, IEEE*

***Abstract*—A radiowave propagation measurement system for wideband multichannel multiple-input–multiple-output (MIMO) measurements at 5.3 GHz is presented. The MIMO channel matrix of size $32 \cdot 32$ can be measured using microwave switches at the transmitter (TX) and the receiver (RX). The system is capable of measuring direction of departure and direction of arrival with a dual polarization in both TX and RX. The antenna configuration can be selected to include a planar array or semispherical groups at each end of the link. A high-power switch is used at TX to enable large measurement distances. Results from a calibration in an anechoic chamber and from the measurement campaigns are shown.**

***Index Terms*—Antenna array, channel sounder, multiple-input–multiple-output (MIMO) measurement, radio channel measurement, radiowave propagation.**

I. Introduction

THE DEVELOPMENT of multiple-input–multiple-output (MIMO) measurement systems is of wide interest. These systems provide the required knowledge about MIMO channels to be used in various areas of research. These areas include basic research of radio wave propagation, antenna research, and multidimensional channel model development. The future wireless networks will be based on the research efforts put into these areas.

A narrowband MIMO measurement system with the matrix size $5 \cdot 7$, where the transmitters (TX) are separated by different frequency shift, was presented in [1]. A wideband MIMO measurement system with matrix size $16 \cdot 32$, where the pseudonoise (PN) coded TX signals are separated by time delay, was presented in [2]. In the receiver (RX), a combination of parallel and multiplexed data acquisition was applied. The MIMO sounder architecture with RF multiplexing in both TX and RX was first presented in [3], developed in Helsinki University of Technology (TKK). The frequency of operation was 2.154 GHz, and the size of the MIMO matrix was $16 \cdot 64$. The MIMO sounder was based on the previously developed single-input–single-output (SISO) sounder [4] using PN-codes, and the RF multiplexing principle, which was introduced in [5] in a single-input–multiple-output (SIMO) measurement configuration. The RF multiplexing was also used in [6], but using a multitone waveform.

Manuscript received June 15, 2005; revised April 20, 2006.

V.-M. Kolmonen, L. Vuokko, and P. Vainikainen are with the Radio Laboratory/Smart and Novel Radios Research Unit (SMARAD), Helsinki University of Technology (TKK), 02015 Espoo, Finland (e-mail: velimatti.kolmonen@tkk.fi; lasse.vuokko@tkk.fi; pertti.vainikainen@tkk.fi).

J. Kivinen was with the Radio Laboratory/SMARAD, Helsinki University of Technology (TKK), 02015 Espoo, Finland. He is now with the Elektrobit OY Teollisuustie 9 A, 02700 Kauniainen, Finland (e-mail: jarmo.kivinen@elektrobit.com).

Digital Object Identifier 10.1109/TIM.2006.877724

The estimation of the wave vector in the RX with full azimuth and elevation range including polarization was first presented in [7] by TKK. The design was based on dual polarized patch antenna elements organized in a spherical geometry. The estimation of the wave vector enables antenna embedding in the data analysis [8]. A different solution based on the dodecahedral array geometry, with monopoles on top of a conducting surface, was presented in [9].

In this paper, a wideband MIMO radio channel measurement system, which is capable of measuring the wave vector in both ends of the radio channel, is presented. The sounder concept is based on the earlier work in [3]–[5], [7], and [8]. The presented system covers three-dimensional (3-D) directions and two orthogonal polarizations of the waves in both RX and TX using $32 \cdot 32$ channels without excessive hardware complexity in the 5.3 GHz frequency range. The link budget and field usability have been demonstrated in practice with several large measurement campaigns in different environments.

Section II presents the conventional beamforming basics used in the simulations. In Section III the hardware realizations and designing steps are presented, followed by measurement system analysis and measurement campaigns in Section IV. Finally, Section V concludes the paper.

II. Directional Measurement by Beamforming

The estimation of the direction of departure (DoD) and the direction of arrival (DoA) can be done by using conventional Fourier processing described in [7]. The processing is based on the phasing of adjacent elements and weighting of the element signals. The angular response of an antenna group[1] with N elements can be written as

$$S(\theta,\phi) = \frac{\sum_{n=1}^{N} \left[h_n(\theta,\phi)s_n + v_n(\theta,\phi)t_n\right] a_n(\theta,\phi)}{\sum_{m=1}^{N} |a_m(\theta,\phi)|} \quad (1)$$

where the phasing of the element n is given by

$$a_n(\theta,\phi) = a_{t,n}(\theta,\phi)e^{-jk\mathbf{r}_n\cdot\mathbf{u}_r t(\theta,\phi)} \quad (2)$$

where $\mathbf{u}_r$ is the scanning unit vector and $a_{t,n}(\theta,\phi)$ is the tapering function. The denominator term a_m in (1) is used to normalize the overall response of the phased antenna group to one. In (1), h_n and v_n are used to take into account the location-dependent orientation of the element polarization, and s_n and

[1] In this paper, the term antenna group is used for general antenna configurations that do not fulfill the condition of an antenna array, where the array factor and the element pattern are separable.

0018-9456/$20.00 © 2006 IEEE

Authorized licensed use limited to: Nile University. Downloaded on March 16,2010 at 09:20:28 EDT from IEEE Xplore. Restrictions apply.

TABLE I
PROPERTIES OF TX AND RX SWITCHES

	TX	RX
Operating center frequency	5.3 GHz	
Bandwidth	±200 MHz	1 – 18 GHz
VSWR	2:1	2:1
Typical Isolation	40 dB	60 dB
Switching speed	2 µs	200 ns
Type	Absorptive	Absorptive
Max input power	10 W	0.8 W
Typical insertion loss	3.5 dB	4 dB (at 5.3 GHz)

t_n are the $\mathbf{u}^{\phi}-$ and $\mathbf{u}^{\theta}-$ polarized signal components of the wave vector $\mathbf{k}_s$

$$\begin{bmatrix} s_n \\ t_n \end{bmatrix} = e^{jk\mathbf{r}_n \cdot \mathbf{u}_r(\theta_s,\phi_s)} \begin{bmatrix} \mathbf{g}_n^{\phi}(\theta_s,\phi_s) \cdot \mathbf{k}_s \\ \mathbf{g}_n^{\theta}(\theta_s,\phi_s) \cdot \mathbf{k}_s \end{bmatrix}. \tag{3}$$

Here, $\mathbf{u}_r(\theta,\phi_s)$ is the direction of the incoming wave, $\mathbf{g}_n^{\phi}$ and $\mathbf{g}_n^{\theta}$ are $\phi-$ and $\theta-$ polarized components of the field pattern, and r_n is the antenna element position vector.

III. HARDWARE REALIZATION

The goal of this paper was to enable estimation of the DoD and DoA including the polarization as completely as possible. However, the MIMO matrix size was limited to $32 \cdot 32$ due to complexity of the hardware, the amount of the measurement data, and the coherence time of the measurement. Separate samplers for different channels could be used, but the parallel architecture and calibration of the parallel branches would increase the complexity. Therefore, in the presented system, microwave switches are used at both the RX and TX. A block diagram of the system is presented in [3]. A combination of the abovementioned parallel and switching architectures is presented in [2].

A. High-Power Switch

The signal-to-noise ratio of the data are of major importance in the data analysis. In channel sounders, the use of separate power amplifiers is not preferable due to their phase fluctuation. On the other hand, the semiconductor-based switches usually cannot handle signals with power more than 1 W. Here, a special high-power switch that can handle 10 W of power was specified and purchased. Thus, the transmit power of 4 W can be used for each channel. Table I presents the main specifications of the TX and RX switches. These switches enable the measurement of $32 \cdot 32$ MIMO matrix in about 8.7 ms.

B. Data Collection and Frame Movement Limits

The amount of data in the I and Q channels (which have separate analog-to-digital (A/D) converters in the sampler of this system) with N and M elements in the antenna groups is

$$N_{\text{byte}} = N \cdot M \cdot 2^2 \cdot L \cdot T_{\text{chip}} \cdot N_{\text{ave}} \cdot f_{\text{sample}} \tag{4}$$

where L is the sequence length ($= 255$), T_{chip} the chip frequency (60 MHz), and N_{ave} the number of averaged impulse responses, which must be at least two, because the switching time has to be discarded from the data. The factor 2^2 comes from the two polarizations at each end. The clock frequency of the A/D converter f_{sample} is 120 MHz. The maximum moving speed is

$$v_{\max} = \frac{\lambda}{n_{\lambda}} \cdot \frac{N_{\text{store}}}{N_{\text{byte}}} \tag{5}$$

where n_{λ} is the number of samples per wavelength ($= 4$ in the following), and N_{store} is the total data storage rate ($= 20$ MB/s) of the I and Q branches. The frame movement during the measurement is another limit. The measurement time of the matrix $T_{\text{matrix}} = N_{\text{byte}}/f_{\text{sample}}$. For example, $N_{\text{byte}} = 1$ MB and $N_{\text{store}} = 20$ MB/s give a maximum speed of $v_{\max} = 5\ \lambda$/s. Then, $T_{\text{matrix}} = 1/120$ s, and the frame movement is $\lambda/24$. In the measurements presented in Section IV, the frame movement was $\lambda/36$, corresponding to a peak-to-peak phase error of 10°.

The samples are stored in two 9 GB hard disks which limit the longest continuous measurement route to about 122 m for the sample distance of $\lambda/4$. The per route measurement data are transferred onto two 30 GB hard disks, which sets the limit for the total measurement route length, before the disks have to be emptied.

C. Group Geometries

In the DoD/DoA measurements, the ideal case would be to be able to cover the whole 4π angle in very short time with a symmetric and narrow beam. A symmetric and narrow beam can be achieved by rotating one antenna towards all the directions. However, this is a very slow measurement technique, and therefore, it is not applicable for mobile measurements. For the current measurement system, due to the switch channel number limitations, some nonidealities had to be allowed, and thus the visibility area had to be reduced from the full 4π. Due to this, and based on the measurement results in [10], the visibility range was defined as 360° in the azimuth and $20° - 120°$ in the elevation.

For possible antenna group geometries under consideration, three geometries were chosen: sphere, cone, and cylinder. Previous studies have shown that the spherical geometry [7] is feasible. The spherical geometry was chosen to contain more antenna elements than there were channels in the switch. This enabled the possibility to use different kind of setups of the geometry and the symmetric structure would minimize the interferences from the adjacent elements. In the future, with a switch with more channels, these elements could also be used to increase the visibility range of the antenna groups.

By using the adjacent element middle point distance $(\lambda/2)$ as the initial design rule, the sizes of the geometries could be determined. The width of the cylinder (using opposite elements) was λ and the height 0.98λ. For the cone the corresponding dimensions were 1.65λ for the width measured from the

Authorized licensed use limited to: Nile University. Downloaded on March 16,2010 at 09:20:28 EDT from IEEE Xplore. Restrictions apply.

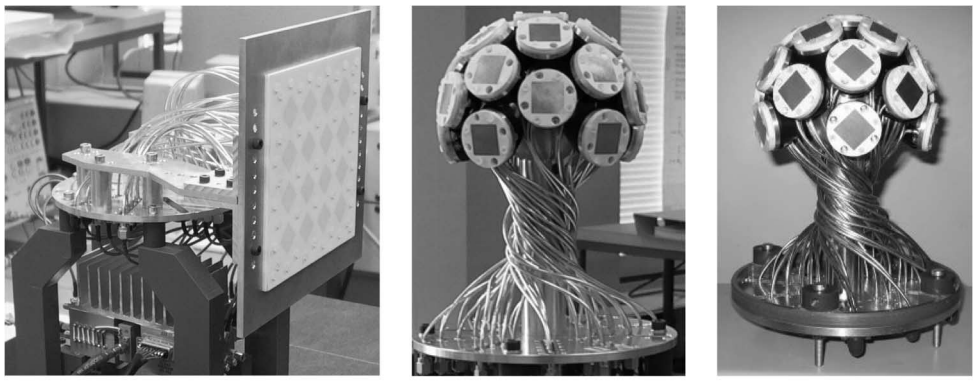

(a) (b) (c)

Fig. 1. Antennas of the sounder. (a) Planar array. (b) Semispherical RX antenna group. (c) Semispherical TX antenna group.

middle of the elements with 20° tilt angle and 0.47λ for the height. The radius of the sphere was chosen to be 0.8λ, which corresponds to the largest neighboring element distance of 0.5λ. The simulations of the geometries were done by using beamforming, as described in Section II. Tapering was not used in the simulations and the element radiation pattern was modeled as a cosine function.

In the simulations, beams were formed into different directions and the width of the main beam was considered. Also, the level and the location of the sidelobes were under consideration. Because of the limited number of channels, it was not reasonable to use all the elements in the spherical geometry, so it was divided into two parts. The first part consisted of 16 top elements (i.e., 32 channels) and the second of 15 (i.e., 30 channels) lowest elements. The chosen division is obvious from the spherical geometry.

From the simulations, it was discovered that the beam of the spherical group remained the most symmetric in the specified angular range, and the sidelobes were clearly below the main beam in its vicinity and thus the results are unambiguous. The beam of the semispherical group is not as symmetric as in [7]; the beam is wider in the elevation plane. This is due to the fact that the aperture of the geometry is more limited in the elevation than in the azimuth.

It was decided to construct two spherical groups. In addition, a 4×4 planar array was ordered to be used as a transmitting antenna in outdoor measurements. In the TX groups, the polarizations of the elements were tilted 45°. Fig. 1 illustrates the final antennas.

The antenna elements were adapted from [7], but they were realized with a substrate with permittivity $\varepsilon_r = 3.48$ to make it possible to place them closely enough. The final design and manufacturing were subcontracted. Table II presents the antenna element specifications.

TABLE II
ANTENNA ELEMENT SPECIFICATIONS

Frequency range	5.2-5.4 GHz
Return loss	10 dB
Polarization discrimination	18 dB
Gain	7 dB
Isolation (d = λ/2)	15 dB
Diameter	30 mm

D. Mechanics

The mechanics had to be designed so that the antenna groups could be changed in both TX and RX ends. Due to this, and the small size of the elements (and small wavelength), special attention had to be paid to the mechanics of the groups. For example, common ground surface could not be constructed in the spherical group. Therefore, the semirigid feed cables of the elements had to be left visible as seen in Fig. 1. The small size of the geometry forced the radius of the sphere to be increased to 0.99λ. A common mechanical interface was constructed for the antenna groups, which can thus be interchanged. The interface was chosen to be a round metal plate, into which the element feed cables were attached. From this plate, the elements can be connected to the switch in an arbitrary order with flexible cables. This doubled the number of cables but enabled the possibility to choose the used elements (i.e., certain channel could be attached to certain channel of the switch), and the groups could be used in either RX or TX. This configuration raises one difficult problem. For an accurate performance, the antenna groups have to be calibrated after each change in the configuration.

To cover the cables and the metallic structure, an absorber was designed under the spherical groups. A metallic cone was constructed to be attached to the round metal plate and the absorber was placed on the top of the cone.

The controlling and the synchronization of the TX switch is performed with a microcontroller, a phase-locked loop and a divider. The TX and RX switches are synchronized in the beginning of a measurement. The synchronization holds for about 2 h in the measurements. For reliability, one channel in TX is disconnected and a load is connected to the switch. Thus, the synchronization can be verified in offline processing.

IV. MEASUREMENTS AND ANALYSIS

The effect of the phase noise to the DoA error of the sounder is analyzed in [11]. Based on that analysis the DoA estimation errors due to the phase noise are less than 1° rms with the

Authorized licensed use limited to: Nile University. Downloaded on March 16,2010 at 09:20:28 EDT from IEEE Xplore. Restrictions apply.

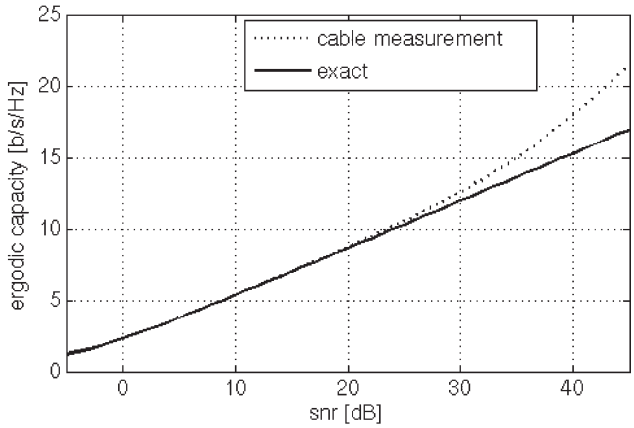

Fig. 2. Ergodic capacity in a 4×4 rank-1 channel subject to channel-sounder nonidealities.

measurement times of the switching groups used in this paper. In [12], it is stated that the switched time domain multiplexing sounder overestimates the capacity of a keyhole case. In Fig. 2, the analysis result of [12] was reproduced with a cable back-to-back measurement for the ergodic capacity of a rank-1 $4 \cdot 4$ MIMO channel. This result includes the effects of the phase noise, thermal noise, quantization noise, nonlinearity of the RX, and the spurious signals in frequency synthesizers. The power amplifier and the switches are bypassed. It is seen that the nonidealities of the sounder are significant in a keyhole case (error more than 1 b/s/Hz) when the signal-to-noise ratio in the analysis of the MIMO capacity is over 33 dB with $4 \cdot 4$ MIMO systems. In the analysis of the field measurement campaigns with significant distance range the signal components below 20-dB dynamic range are generally considered to be negligible. Therefore, the sounder data are reliable in predicting MIMO performance with realistic signal-to-noise ratios.

A. Measurement System Analysis

Full 3-D radiation patterns of the antenna elements of the antenna groups in Fig. 1 were measured in an anechoic chamber. The measurement system was constructed inside of the chamber as SIMO or multiple-input–single-output (MISO) configuration depending on the antenna group. For the RX semispherical antenna group, a dual-polarized high-quality Vivaldi antenna was used as TX antenna. For the TX semispherical antenna group and for the planar antenna array, the same Vivaldi antenna was used as RX antenna. The antenna groups were rotated enabling the measurement of full 4π angle for all channels.

The 4π angular range was sliced into vertical cuts with an automatic rotation and the azimuth angle was manually changed between sweeps. The elevation measurement points were determined by setting the triggering time of the measurement system according to the antenna rotation speed. Since the measurement was performed using the full measurement system, the delay domain of the measurement can also be utilized if needed. This type of calibration measurements can be used for system accuracy analysis [13], but they are also needed for measurement data postprocessing, like space-alternating generalized expectation-maximization (SAGE) [14] parameter estimation.

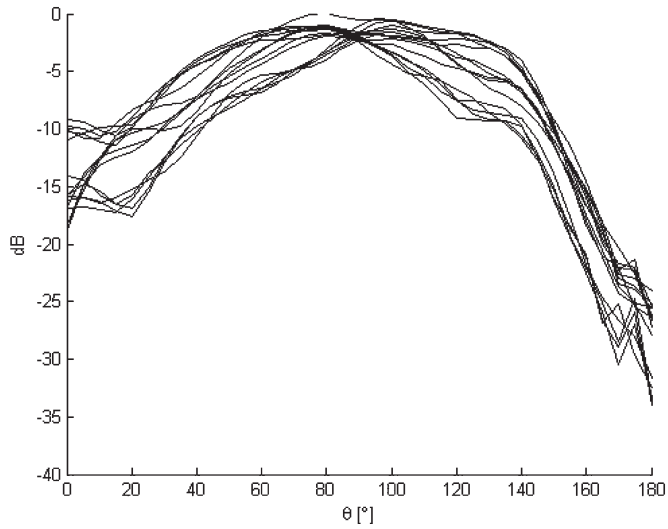

Fig. 3. Vertical cut of vertical radiation patterns.

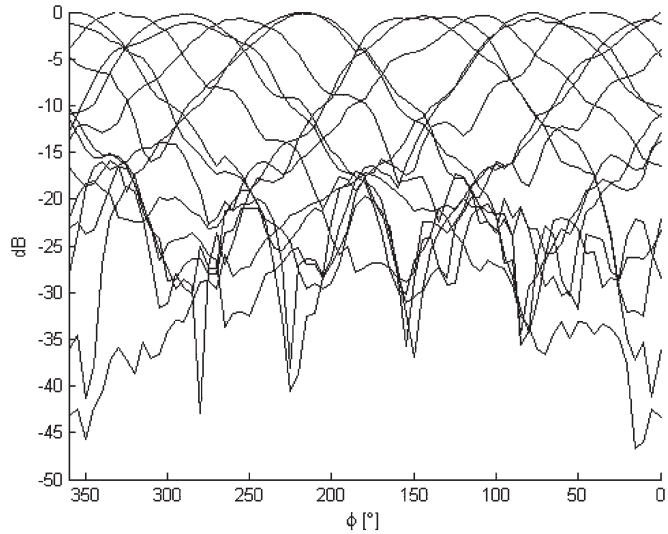

Fig. 4. Horizontal cut of horizontal radiation patterns.

Figs. 3 and 4 present the normalized vertical and the horizontal cuts of the radiation patterns of the RX semispherical antenna group using the 15-element configuration. From Fig. 3 it can be noted that, based on 3-dB beamwidths of the elements, this configuration can be used to measure the elevation range of $40^\circ - 120^\circ$ and the full azimuth range of 360°. Fig. 5 illustrates a beamforming result from anechoic chamber measurement for one direction using the 15 element configuration of the RX group. As already noted in Section III, the beam of the group is not symmetric. The 3-dB beamwidths of the group can be estimated from the beamforming result of the measurement to be approximately 44° and 26° in elevation and azimuth, respectively. The sidelobe level (SLL) of the pattern is about -12 dB.

The beamforming was performed according to (1). The used tapering function in (2) is given by

$$a_{t,n}(\mathbf{u}_r) = \mathbf{r}_n \cdot \mathbf{u}_r \tag{6}$$

where negative values of $a_{t,n}(\mathbf{u}_r)$ are set to zero. This tapering is less abrupt compared to that used in [7].

Authorized licensed use limited to: Nile University. Downloaded on March 16,2010 at 09:20:28 EDT from IEEE Xplore. Restrictions apply.

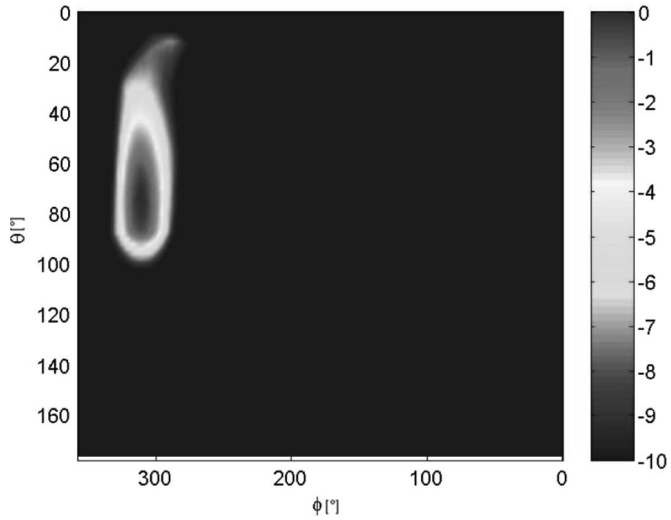

Fig. 5. Semispherical group response in an anechoic chamber.

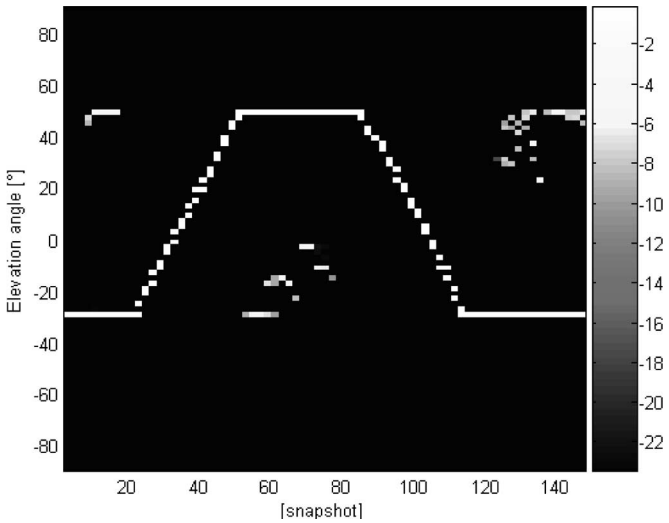

Fig. 6. Estimated elevation angle in an anechoic chamber measurement.

The accuracy of the measurement system in the spatial domain was considered from one continuous vertical measurement sweep in one azimuth angle. Figs. 6 and 7 present the beamforming results for the RX semispherical array. Components more than 20 dB below the maximum component have been cut off. Figures are produced so that at each measurement point, impulse responses between all antenna element pairs are measured by creating a snapshot for a certain direction. These impulse responses are processed with the beamforming algorithm tap independently with an angular grid of 2°. For each snapshot, the local maxima of the spatial response are recorded and plotted in the figures (i.e., different delay components are summed).

From Figs. 6 and 7, we can see that the semispherical array produces very good results within the operation range. Spurious responses emerge outside of the operation range due to the fact that the processing is forced to the operating region.

Based on computational tests using the calibration measurements, this single wave evaluation also applies to the multiple wave scenario where the time of arrival (ToA) of the waves

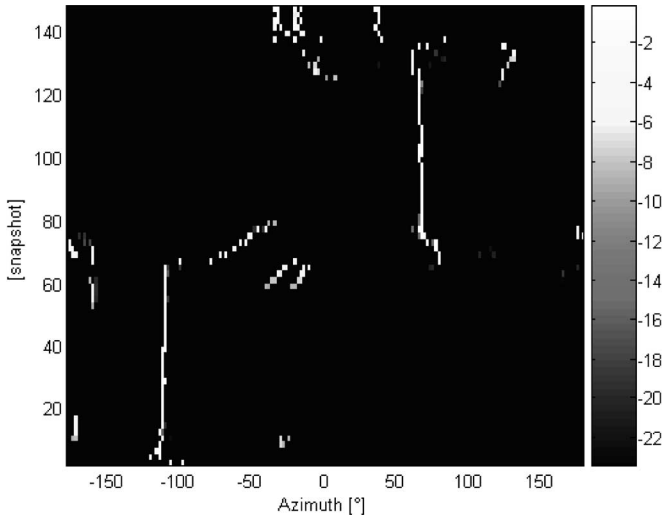

Fig. 7. Estimated azimuth angle in an anechoic chamber measurement.

TABLE III
MEASUREMENT SYSTEM PARAMETERS VP

	sph RX	sph TX	plan TX
Azimuth direction error	1.69° rms	1.34° rms	0.86°
Elevation direction error	2.38° rms	2.40° rms	1.94°
Mean XPD	21.62 dB	22.53 dB	21.90 dB
Phase ripple	9.9° p-p	11.63° p-p	

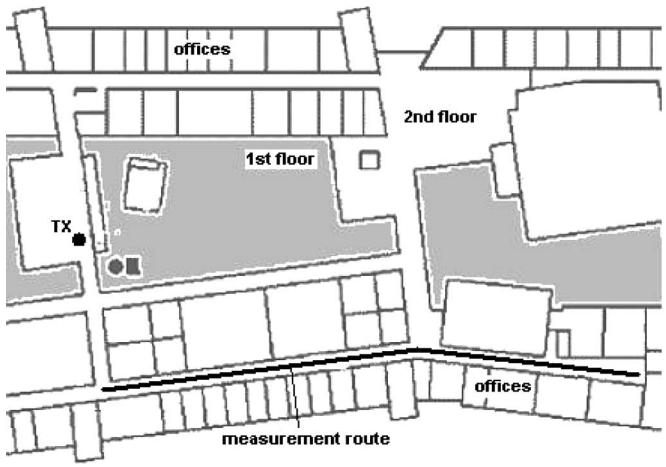

Fig. 8. Map of the measurement environment.

are separated more than $T_{\mathrm{chip}} \sim 17$ ns corresponding to $\sim$ 5-m difference in path length. If the waves arrive within T_{chip}, the traditional performance of the DoA estimation is defined by the beamwidths mentioned earlier.

Table III presents the anechoic measurement results for the RX and TX semispherical antenna groups. Here, we considered only the region of operation with vertical polarization (VP).

The semispherical antenna groups perform very much as expected. The cross polarization discrimination (XPD) values of all the antenna groups are at the same level even though the

Authorized licensed use limited to: Nile University. Downloaded on March 16,2010 at 09:20:28 EDT from IEEE Xplore. Restrictions apply.

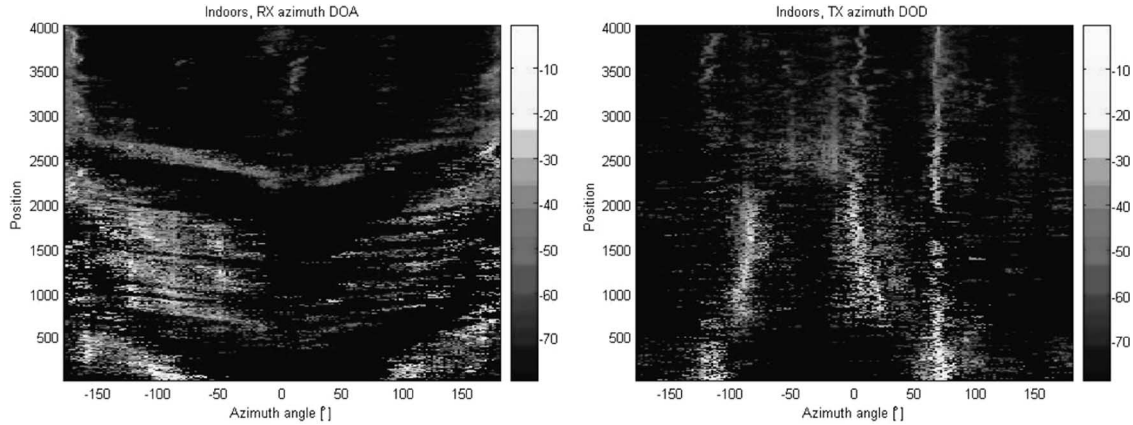

Fig. 9. Azimuth DoA and DoD distributions in an indoor measurement.

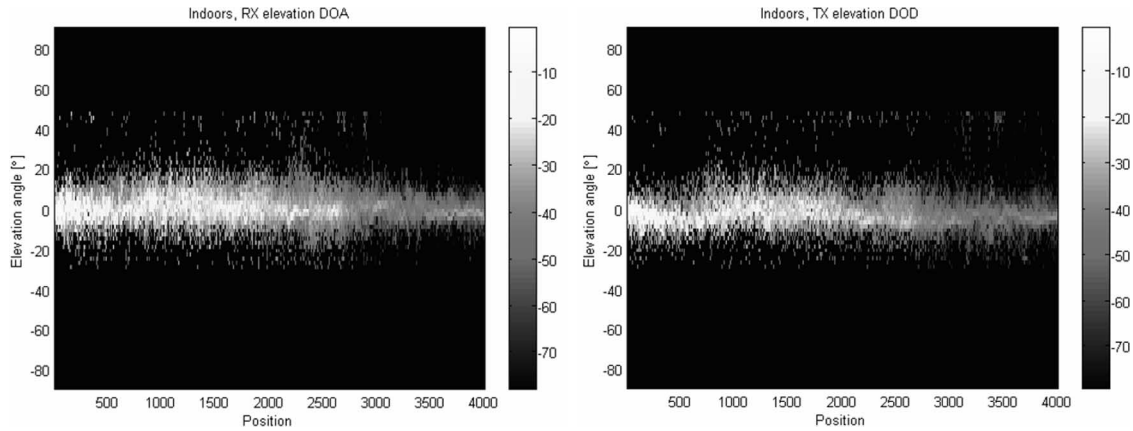

Fig. 10. Elevation DoA and DoD distributions in an indoor environment.

TX antenna groups have slanted elements, i.e., all the elements have some component of the vertically polarized wave in both channels.

For the semispherical antenna groups, the rms error of the azimuth direction estimation is about 1.5 and elevation almost 3.5 times larger than in [7], where the direction estimation error was of the same order in both directions. The two most significant components of the error are the quantization error from the angular grid of 2° and the smaller number of elements than in [7]. The SLL is 1 dB lower than in [7] even though the tapering function used here is less abrupt. This suggests that the tapering could be made tighter to decrease the SLL. This, however, would widen the beamwidths and decrease the spatial resolution.

B. Measurement Campaigns

The system has been used in several measurements in micro, macro, outdoor–indoor, and indoor environments. The total length of the measurement routes is over 2 km and the largest measurement distance in the macro measurements has been over 500 m in nonline-of-sight (NLOS) cases. Measurements have been performed with different RX and TX antenna configurations, such as planar–semispherical and semispherical–semispherical. In some microcell measurements, the TX array was swept vertically on a crane while the RX semispherical group was held static. Here, we present some DoD and DoA results from the indoor measurements where two semispherical groups were used.

The measurements were performed at the TKK campus area in two buildings, namely the Electrical and Communications Engineering (ECE) and the Computer Science and Engineering (CSE) department buildings. The TX antenna was located in coffee rooms in laboratory wings in ECE and CSE, in an office corridor in CSE, and on a bridge crossing the main hall of the CSE building at second-floor height. The TX antenna group was the semispherical antenna group with slanted elements [Fig. 1(c)]. The RX was moved in corridors and nearby office rooms to measure an indoor environment. The total length of the measurements was $\sim$ 500 m ($\sim$ 33 000 snapshots).

Figs. 9 and 10 present the separately estimated DoD and DoA distributions for one indoor measurement from the CSE building. The map of the environment is shown in Fig. 8.

The indoor propagation phenomena can clearly be seen in the results. In the beginning of the route, the main radio wave component is coming directly from left-hand side of the RX, i.e., $-90°$. As the trolley is moved along the corridor, the impinging angle of the main component of the radio propagation channel is decreased according to the corridor corner. Another similar phenomenon can be seen near the second crossing corridor. First, the wave arrives from the front of the RX. As the RX crosses the corridor, the impinging angle of the wave changes accordingly.

Authorized licensed use limited to: Nile University. Downloaded on March 16,2010 at 09:20:28 EDT from IEEE Xplore. Restrictions apply.

V. Conclusion

This paper presents a measurement system that can measure directional data including polarization in both ends of the link with relatively small size antenna groups with semispherical and planar shapes. The elevation range is limited to $40^\circ - 120^\circ$ with the current setup in which the directional rms errors are within $1^\circ - 2.5^\circ$ when the conventional beamforming is used. The incoming waves with ToA difference of less than 17 ns can be separated in the spatial domain with beamforming if their angular separation is larger than 44° and 26° in elevation and azimuth direction. The mean XPD value for the antennas is approximately 20 dB. A high-power TX switch is used to enable measurement distances of over 500 m in NLOS macro cellular environments. The measurement system has been used for measurements of total length over 2 km in various environments. The measurement campaigns have confirmed the system to be usable and reliable for mobile field measurements.

The measurement data can be used for joint DoD and DoA estimation using advanced methods like SAGE, for studying antenna performance by convolving measured radiation patterns with the DoD and DoA data [15], for modeling of MIMO radio channel (empirical, semiempirical), and for studying radio wave propagation mechanisms.

References

[1] M. J. Gans, N. Amitay, Y. S. Yeh, X. Hao, T. C. Damen, R. A. Valenzuela, T. Sizer, R. Storz, D. Taylor, W. M. MacDonald, T. Cuong, and A. Adamiecki, "Outdoor BLAST measurement system at 2.44 GHz: Calibration and initial results," *IEEE J. Sel. Areas Commun.*, vol. 20, no. 3, pp. 570–583, Apr. 2002.

[2] J. B. Andersen, J. Ø. Nielsen, G. F Pedersen, K. Olesen, P. Eggers, E. H. Sørensen, and S. Denno, "A 16 by 32 wideband multichannel sounder at 5 GHz for MIMO," in *Proc. IEEE Int. Antennas Propag. Symp. and USNC/URSI Nat. Radio Sci. Meeting*, Jun. 20–26, 2004, pp. 1263–1266.

[3] J. Kivinen, P. Suvikunnas, D. Perez, C. Herrero, K. Kalliola, and P. Vainikainen, "Characterization system for MIMO channels," in *Proc. 4th WPMC*, Aalborg, Denmark, Sep. 9–12, 2001, pp. 159–162.

[4] J. Kivinen, T. Korhonen, P. Aikio, R. Gruber, P. Vainikainen, and S.-G. Häggman, "Wideband radio channel measurement system at 2 GHz," *IEEE Trans. Instrum. Meas.*, vol. 48, no. 1, pp. 39–44, Feb. 1999.

[5] K. Kalliola and P. Vainikainen, "Characterization system for radio channel of adaptive array antennas," in *Proc. IEEE 8th PIMRC—Waves of the Year 2000*, Sep. 1–4, 1997, vol. 1, pp. 95–99.

[6] R. S. Thomä, D. Hampicke, A. Richter, and G. Sommerkorn, "MIMO vector channel sounder measurement for smart antenna system evaluation," *Eur. Trans. Telecommun.—Special Issue on Smart Antennas*, vol. 12, no. 5, pp. 427–438, Sep.–Oct. 2001.

[7] K. Kalliola, H. Laitinen, L. Vaskelainen, and P. Vainikainen, "Real-time 3-D spatial temporal dual-polarized measurement of wideband radio channel at mobile station," *IEEE Trans. Instrum. Meas.*, vol. 49, no. 2, pp. 439–448, Apr. 2000.

[8] K. Sulonen, P. Suvikunnas, L. Vuokko, J. Kivinen, and P. Vainikainen, "Comparison of MIMO antenna configurations in picocell and microcell environments," *IEEE J. Sel. Areas Commun.*, vol. 21, no. 5, pp. 703–712, Jun. 2003.

[9] J. Verhaevert, E. Van Lil, and A. Van de Capelle, "Three-dimensional monopole antenna for direction of arrival determination," *Proc. Inst. Elect. Eng.,—Microw. Antennas Propag.*, vol. 151, no. 2, pp. 121–126, Apr. 2004.

[10] K. Kalliola, K. Sulonen, H. Laitinen, O. Kivekäs, J. Krogerus, and P. Vainikainen, "Angular power distribution and mean effective gain of mobile antenna in different propagation environments," *IEEE Trans. Veh. Technol.*, vol. 51, no. 5, pp. 823–838, Sep. 2002.

[11] J. Kivinen and P. Vainikainen, "Calibration scheme for synthesizer phase fluctuations in virtual antenna array measurements," *Microw. Opt. Technol. Lett.*, vol. 26, no. 3, pp. 183–187, Aug. 2000.

[12] D. Baum and H. Bölcskei, "Impact of phase noise on MIMO channel measurement accuracy," in *Proc. IEEE VTC—Fall*, Los Angeles, USA, Sep. 26–29, 2004, pp. 1614–1618.

[13] M. Mustonen, P. Suvikunnas, and P. Vainikainen, "Reliability analysis of multidimensional propagation channel characterization," in *Proc. 8th WPMC*, Aalborg, Denmark, Sep. 18–22, 2005, vol. 1, pp. 534–537.

[14] J. A. Fessler and A. O. Hero, "Space-alternating generalized expectation-maximization," *IEEE Trans. Signal Process.*, vol. 42, no. 10, pp. 2664–2677, Oct. 1994.

[15] P. Suvikunnas, K. Sulonen, J. Villanen, C. Icheln, J. Ollikainen, and P. Vainikainen, "Evaluation of performance of multi-antenna terminals using two approaches," in *Proc. IEEE 21st IMTC*, May 18–20, 2004, vol. 2, pp. 1091–1096.

Veli-Matti Kolmonen was born in Rovaniemi, Finland, in 1979. He received M.Sc. degree in technology from Helsinki University of Technology (TKK), Espoo, Finland, in 2004.

Since 2003, he has been with the Radio Laboratory, TKK, first as a Research Assistant and later as a Researcher. His current research interests include radio channel measurements and modeling.

Jarmo Kivinen was born in Helsinki, Finland, in 1965. He received the M.Sc., Lis.Sc., and Dr.Sc. degrees in technology from Helsinki University of Technology (TKK), Espoo, Finland, in 1994, 1997, and 2001, respectively, all in electrical engineering.

He worked as a Research Engineer and Project Leader at the Radio Laboratory of TKK from 1994 to 2005 and as an RF Design Engineer at Nokia Telecommunications from 1995 to 1996. Since 2006, he has been working as a Specialist at Elektrobit OY, Kauniainen, Finland. His main fields of interest are multidimensional radio propagation channel measurement and modeling techniques and RF techniques in radio communications.

Lasse Vuokko was born in Vantaa, Finland, in 1977. He received the M.Sc. and Lis.Sc. degrees in technology from Helsinki University of Technology (TKK), Espoo, Finland, in 2001 and 2006, respectively.

Since 1999, he has been with the Radio Laboratory, TKK, first as a Research Assistant and later as a Researcher. During 2002–2003, he was visiting Tokyo Institute of Technology, Tokyo, Japan. His current research interests include mobile-radio propagation and radio-channel measurements.

Pertti Vainikainen (S'84–M'90) received the M.Sc., Lis.Sc., and Dr.Sc degrees in technology from Helsinki University of Technology (TKK), Espoo, Finland, in 1982, 1989, and 1991, respectively.

From 1992 to 1993, he was an Acting Professor of radio engineering; since 1993, he has been an Associate Professor of radio engineering; and since 1998, he has been a Professor in radio engineering, all in the Radio Laboratory of TKK. In 1993–1997, he was the Director of the Institute of Radio Communications (IRC) of TKK and, in 2000, a Visiting Professor at Aalborg University, Aalburg, Denmark. He is the author or coauthor of six books and about 240 refereed international journal or conference publications and the holder of seven patents. His main fields of interest are antennas and propagation in radio communications and industrial measurement applications of radio waves.

Authorized licensed use limited to: Nile University. Downloaded on March 16,2010 at 09:20:28 EDT from IEEE Xplore. Restrictions apply.